# UC San Diego

## UC San Diego Previously Published Works


### Title

Perfluorocarbon-loaded polydopamine nanoparticles as ultrasound contrast agents


### Permalink

https://escholarship.org/uc/item/2ws1f6mt



### Journal

Nanoscale, 10(26)

### ISSN

2040-3364



### Authors

Xie, Yijun

Wang, James

Wang, Zhao

et al.



### Publication Date

2018-07-09

### DOI

10.1039/c8nr02605j

Peer reviewed



eScholarship.org Powered by the California Digital Library
University of California

Author Manuscript

Author Manuscript

Author Manuscript

Author Manuscript

HHS Public Access

Author manuscript

*Nanoscale*. Author manuscript; available in PMC 2019 July 09.

Published in final edited form as:

*Nanoscale*. 2018 July 09; 10(26): 12813–12819. doi:10.1039/c8nr02605j.

# Perfluorocarbon-loaded polydopamine nanoparticles as ultrasound contrast agents

**Yijun Xie**[a,b], **James Wang**[a,c], **Zhao Wang**[a,d], **Kelsey A. Krug**[a], and **Jeffrey D. Rinehart**[a,b]

[a]Department of Chemistry and Biochemistry, University of California, San Diego, La Jolla, CA 92093, USA, jrinehart@ucsd.edu

[b]Materials Science and Engineering Program, University of California, San Diego, La Jolla, CA 92093, USA.

[c]Department of NanoEngineering, University of California, San Diego, La Jolla, CA 92093, USA.

[d]Department of Chemistry, Northwestern University, Evanston, IL 60208, USA

## Abstract

A versatile platform for the development of new ultrasound contrast agents is demonstrated through a one-pot synthesis and fluorination of submicron polydopamine (PDA-F) nanoparticles. The fluorophilicity of these particles allows loading with perfluoropentane (PFP) droplets that display strong and persistent ultrasound contrast in aqueous suspension and ex vivo tissue samples. Contrast under continuous imaging by color Doppler persists for 1 h in 135 nm PDA-F samples, even at maximum clinical imaging power (MI = 1.9). Additionally, use of a Cadence Contrast Pulse Sequence (CPS) results in a non-linear response suitable for imaging at 0.5 mg/mL. Despite the PFP volatility and the lack of a hollow core, PDA-F particles display minimal signal loss after storage for over a week. The ability to tune size, metal-chelation, and add covalently-bound organic functionality offers myriad possibilities for extending this work to multimodal imaging, targeted delivery, and therapeutic functionality.

## Introduction

Medical ultrasound imaging is an essential modern diagnostic technique due to its affordability, lack of ionizing radiation, portability, tissue penetration, and real-time display. It serves as a valuable complement to more costly imaging modalities such as magnetic resonance imaging (MRI), positron emission tomography (PET), and computed tomography (CT).[1–3] As in many other medical imaging methods, ultrasound can be enhanced through the introduction of a contrast agent. These agents generate contrast against surrounding tissue via a non-linear resonance interaction with the impinging ultrasound waves and thus do not require magnetic or radioactive properties to achieve strong signal to noise ratios. In

Conflicts of interest

There are no conflicts to declare.

[†]Footnotes relating to the title and/or authors should appear here.

Electronic Supplementary Information (ESI) available: [details of any supplementary information available should be included here]. See DOI: 10.1039/x0xx00000x

Author Manuscript Author Manuscript Author Manuscript Author Manuscript

fact, the current clinically-employed ultrasound agents are all inert low-boiling perfluorocarbons (PFC) stabilized within simple phospholipid or protein coatings.[2, 4] Under ultrasonic stimulation, these PFC droplets undergo large pressure changes resulting in a transition to a gaseous microbubble which can provide contrast under various ultrasound modalities.[5] Additionally, these microbubbles can potentially re-condense and provide long-term imaging through subsequent cavitational oscillations.[6] The large size of current ultrasound contrast agents (1–5 μm) is advantageous because it allows for high PFC-loading; however, it also restricts particle circulation time, displays poor accumulation and retention in target tissues, and only generates strong contrast at low frequencies, thus limiting resolution.[6] To improve upon these properties, a range of inorganic ultrasound contrast agents have been developed with better size control including hollow/porous silica,[1, 7–15] carbon nanotubes,[16] calcium carbonate nanoparticles,[17] and others.[18, 19] The rigid shell structure of these materials allows for robust particles of sub-micron diameter and can encapsulate PFC in a more stable fashion. While structurally versatile, many inorganic contrast agents have limited size tunability due to the need for thin shells, and, in some cases, biocompatibility is limited or unknown. Ideally, an ultrasound contrast agent combines the biocompatibility of commercial organic structures with the structural versatility of the inorganic materials. One such approach is with polymer nanoparticles such as polydopamine (PDA), which is structurally very similar to naturally occurring melanin.[20] Many studies have demonstrated the biocompatibility of PDA, and coatings of PDA are frequently used to enhance the biocompatibility of other materials.[21–23] Furthermore, the chemical functionality present in PDA allows for a range of modifications via covalent bond formation and metal chelation leading to applications in MRI contrast,[21, 24–27] drug delivery,[28] cell imaging,[29] and photothermal therapeutics.[30, 31] It is also tolerant of acidic and basic environments, forms stable aqueous suspensions, and can be synthesized at sub-micron sizes. While it lacks native ultrasound contrast and it is neither porous or fluorophilic enough to encapsulate or adsorb PFC, functionalization with fluorinated molecules has been demonstrated to facilitate the uptake of PFC in other polymer nanoparticles.[32–34] Herein, we demonstrate that < 0.5 μm fluorine-functionalized PDA nanoparticles (PDA–F NPs) are capable of stabilizing perfluoropentane (PFP, b.p. = 29.2 C) droplets under aqueous conditions for use in color Doppler and cadence contrast pulse sequencing (CPS) ultrasound imaging.

## Results and discussion

Without significant porosity or fluorophilicity, PDA is predicted to show minimal uptake of PFCs and therefore minimal ultrasound contrast. Control samples of fluorine-free PDA were synthesized by previously described methods. Briefly, dopamine was dissolved in the mixture of ethanol and water under alkaline conditions and allowed to react for 24 h with stirring.[35] The dopamine polymerization process is briefly described in Scheme S1. Typical transmission electron microscopy (TEM) and scanning electron microscopy (SEM) images are shown in Fig. 1 and Fig. S1. By varying the dopamine hydrochloride (DA) concentration of the starting solution, particles of 74±10, 174±28, and 350±40 nm (PDA-74, PDA-174, and PDA-350, respectively) were obtained as determined by transmission electron microscopy (TEM) (Fig. 1(a-c)). Fluorine-functionalized PDA (PDA-F) NPs were similarly

Author Manuscript Author Manuscript Author Manuscript Author Manuscript

prepared with the only variation being an *in situ* Michael addition reaction commonly shown to functionalize catechols with thiol and amino groups under mild alkaline conditions.[31, 36, 37] Specifically, perfluorodecanethiol was added after 9 h of reaction time such that the growing PDA incorporated the perfluorinated side-chain as has been demonstrated previously for the synthesis of superhydrophobic surfaces.[38, 39] PDA-F NPs of 41±14, 135±28, and 242±33 nm PDA-F (PDA-41-F, PDA-135-F, and PDA-242-F, respectively) were synthesized to allow comparison to unfluorinated PDA of roughly equivalent size (Fig. 1(d-f); Fig. S1(d-f), Supporting information). The presence of C–F bonds at the particle surface was confirmed by X-ray photoelectron spectroscopy (XPS) on all three PDA-F samples.[40] (Fig. S2). Energy dispersive X-ray spectra (EDS) was used to quantify S and F content of PDA-F NPs (Fig. S3). PDA-135-F and PDA-242-F show ~8 wt% F with a S ratio roughly corresponding to that expected for the perfluorodecanethiol unit. However, PDA-41-F has far higher F and S content, consistent with the low-density interparticle linking structures visible by TEM. Interestingly, direct addition of perfluorodecanethiol prior to PDA nucleation did not result in any particle formation, likely due to excessive termination of the polymer growth sites by the thiol.

Alterations in the particle morphology between PDA and PDA-F can be observed by TEM, with interparticle polymericlinkages clearly forming in the case of PDA-41-F. To examine the extent of these linkages, Dynamic Light Scattering (DLS) was employed to determine the average hydrodynamic radius ($R_{hyd}$) of PDA-41-F ($R_{hyd}$ = 220 nm), PDA-135-F ($R_{hyd}$ = 250 nm), and PDA-242-F ($R_{hyd}$ = 400 nm) suspensions. These results corroborate the TEM data wherein PDA-41-F displays significant covalent interparticle linkage while both PDA-135-F and PDA-242-F show little to no linkage or aggregation (Fig. S4). Zeta potentials of PDA-41-F, PDA-135-F, and PDA-242-F were −9.6±1.3, −13.7±0.7 and −23.8±1.4 mV, respectively, showing moderate stability in aqueous solution. Even the largest of our particles are significantly smaller than current clinical ultrasound contrast agent sizes ($R_{hyd}$ = 1−7 μm)[41] thus increasing their potential for cell permeability and use in extravascular space.

To function as an ultrasound contrast agent, PDA-F requires enough fluorophilicity to nucleate a liquid droplet of low boiling point PFC. Similar to other ultrasound agents, PDA-F can then generate contrast from a phase shift of the probe ultrasound pulse. Uniquely, our PFC droplet is external to the stabilizing unit (PDA-F) instead of being encapsulated by it as in all other ultrasound agents reported to date. Loading of PDA-F with perfluoropentane (PFP, $T_b$ = 29.2 °C) was achieved by suspending the NPs in 200 μL of PFP liquid, sonicating for 30 s, and allowing the residual to evaporate. Dynamic Light Scattering (DLS) data of PFP-loaded PDA-F demonstrates an increase in hydrodynamic radius size compared with pure PDA-F samples, consistent with PFP-loading on the surface (Fig. S5).

Subsequent to exposure to PFP, both PDA and PDA-F samples were examined using two ultrasound imaging modes: Color Doppler and Contrast Pulse Sequencing (CPS). Unlike standard B mode imaging, CPS does not show contrast in the absence of an effective contrast agent and color Doppler will only show contrast in a flowing medium. Color Doppler signal is a result of cavitation and release of PFP gas which can then be imaged as blue- or redshifted signal from the moving gas.[8] Color Doppler imaging was performed on

Author Manuscript Author Manuscript Author Manuscript Author Manuscript

stable aqueous suspensions of 0.5 mg/mL PDA and PDA-F at an optimized frequency ($f$ = 7 MHz) with a clinically-safe Mechanical Index (MI ≤ 1.9). Color Doppler of PDA-F reveals a far stronger response than the unfluorinated PDA NPs (Fig. 2a-c). The drastic increase in signal upon fluorination of the polymer NPs indicates a much higher uptake of PFP in PDA-F samples. Control experiments on aqueous dispersions of 0.5 mg/mL PDA-74, PDA-174 and PDA-350 without PFP treatment reveal that pure PDA particles do not show color Doppler signal above background (Fig. S6).

One factor of particular importance in color Doppler imaging is the temporal persistence of signal. We found that all three PDA-F sizes show significant color Doppler signal persistence (Fig. 2d-f), with PDA-135-F providing approximately 1 h of imaging time (Fig. 3d and Fig. S7). Although the color Doppler signal is difficult to quantify, continuous imaging for 1 h is not achievable with current commercial ultrasound contrast agents.[7, 42] By comparison, commercially-available Definity samples (Perflutren Lipid Microspheres) retain a color Doppler signal for approximately 5 min (Fig. S7c).

Given the long imaging times, testing of stability of PFC loading allows for delayed imaging and periodic imaging without reintroduction of contrast agent. To demonstrate the long-term stability of PFP-loaded PDA-F particles, PDA-135-F was charged with PFP and stored at 4 °C for one week. Color Doppler imaging reveals a strong signal roughly equivalent to that of freshly prepared samples (Fig. 4).

To provide a more quantitative analysis of the ultrasound contrast ability of pure PDA and PDA-F NPs, CPS imaging was performed as a function of MI (Fig. 5). CPS signal is achieved via a non-linear response designed to improve specificity to the contrast agent. CPS brightness quantification was adapted from Liberman *et al.*[43] Briefly, the gold specks in the CPS correspond to echo decorrelation events and signal generation from PFP gas. An average brightness was determined from the signal intensity of a fixed region of interest. In parallel to the color Doppler results, PDA-F demonstrates strong contrast compared to unfluorinated PDA samples (Fig. 5). In fact, there is no significant contrast difference between PDA samples and deionized water (Fig. S8), confirming PFP as the source of the CPS contrast. Unlike commercial ultrasound agents, the CPS signal was found to increase continuously with increasing MI, up to 1.9. These results indicate the robust nature of PFP adhesion to PDA-F NPs, despite its volatility. Particles of the intermediately-sized PDA-135-F shows the highest contrast intensity among three PDA-F samples, with approximately twice the brightness of PDA-41-F and PDA-242-F (Fig. 3a-c). The CPS signal of our PDA-F is also comparable to the commercial agent Definity (Fig. S9) as well as promising new contrast agents such as perfluorocarbon-loaded hollow silica.[8] We also note that quantitative CPS analysis (Fig. 4c) shows that after one-week, PDA-135-F particles still retain 96% of the brightness of freshly prepared samples (Fig. 4b).

To investigate whether the morphology of PDA-F was impacted by ultrasound imaging, TEM images were collected of the samples after ultrasound imaging at MI = 1.9 immediately. Although aggregation is observed, the PDA-F NPs remain intact, with no evidence of broken or deformed particles (Fig. 6).

Author Manuscript Author Manuscript Author Manuscript Author Manuscript

PDA has been demonstrated to be a robust material under a wide range of conditions, including those relevant to *in vivo* ultrasound. In fact, natural melanin is a ubiquitous polymeric biomaterial that shares many structural characteristics with PDA. Preliminary *in vitro* cytotoxicity of PDA-41-F, PDA-135-F, and PDA-242-F ($c$ = 10 to 500 μg/mL) was assessed by incubation with HCT116 cells for 24 h. Analysis via MTS ((3-(4,5-dimethylthiazol-2-yl)-5-(3-carboxymethoxyphenyl)-2-(4-sulfophenyl)-2H-tetrazolium)) assay indicates cell viability greater than 90% for all samples at all concentrations (Fig. S10).

As an additional probe of the biological stability and bioimaging capability of PDA-F, an *ex vivo* imaging study was performed in fresh porcine liver tissue (Fig. 7). Liver tissue was chosen because hepatic clearance plays a major role in nanoparticle biomedical applications.[44] Furthermore, liver is highly vascularized and can be used as an easily accessible preliminary demonstration for tissue compatibility of the PDA nanoparticles. PDA-F was injected 2 cm into three separate tissue locations and immediately imaged via color Doppler, giving signal persistence roughly equivalent to that observed *in vitro*. It has been demonstrated that at an MI of 1.9, PDA-F was visible via color Doppler at up to 2 cm tissue depth. Although commercial microbubbles usually operate at a lower MI via bubble oscillation, the PDA-F nanoparticles generated ultrasound signal from surface condensed PFP that was phase changed under ultrasound insonation, which may require a higher ultrasound pressure (MI = 1.9). Nevertheless, the unique mosaic pattern of the color Doppler signal generated from the PDA-F remains an obvious contrast to B-mode ultrasound signal from the liver tissue. The signal footprint on the Doppler graph was on average 4 $cm^3$, (40 times the initial injection volume of 100 μL), demonstrating effective tissue perfusion in the liver. Additionally, *in vivo* blood flow patterns typically exhibit solid color Doppler signals due to their fixed directional flow. As a result, PDA-F perfused tissue, or potentially tumors, can be easily identified via ultrasound imaging.

## Conclusions

Perfluorodecanethiol-functionalized PDA NPs (PDA-F NPs) have been demonstrated to load the perfluorocarbon PFP and function as stable, bright, long-lived contrast agents in two clinically-relevant ultrasound modalities: Color Doppler and CPS. A series of PDA-F NPs with size from 70 nm to 350 nm were synthesized with 170 nm PDA-F NPs demonstrating the best signal to noise ratio and longevity. Compared with commercial contrast agents, PDA-135-F NPs show favorable color Doppler imaging lifetime (~1 h) and comparable CPS signal, despite being volumetrically two orders of magnitude smaller. Even more intriguing may be their facile synthetic tunability. Not only does this offer the possibility to improve upon their contrast characteristics, but also (1) size can be tuned across a wide range allowing for variable extravasation, passive targeting of cells, and increased retention time, (2) surface functionality can be tuned to allow specific targeting of biomolecules in vivo, and (3) chelation of metals at the catechol units of PDA can be tuned to install multi-functionality such as MRI contrast.[21, 24–27]

Author Manuscript Author Manuscript Author Manuscript Author Manuscript

## Experimental

### Materials

Dopamine hydrochloride (99%) and Tris(hydroxymethyl)aminomethane (Tris, 99%) were purchased from Alfa Aesar. 1H,1H,2H,2H-Perfluorodecanethiol (97%) was purchased from Sigma-Aldrich. Perfluoropentane (PFP) was purchased from Strem Chemicals. Ethanol (100%) was obtained from Fisher Scientific. All chemicals and solvents were used without further purification. Fresh pork liver for ex vivo tissue imaging was purchased from 99 Ranch Market and used as received.

### Characterization

TEM images were collected on an FEI Tecnai G2 Spirit TEM operating at 120 kV. SEM images and elemental composition were collected on an FEI Quanta 250 SEM equipped with a Thermo Fisher Scientific Energy-dispersive X-ray spectroscopy (EDS) detector. Size of dispersed PDA and PDA-F nanoparticles in aqueous solution and zeta potentials were determined by Dynamic Light Scattering (DLS) measured with a Malvern Zetasizer Nano ZS90. XPS data were collected on a Thermo Scientific ESCALAB 250 Xi spectrometer using monochromated Al Kα radiation. The carbon 1s peak at 284.8 eV was used for calibration. Ultrasound data were collected on a Siemens Sequoia 512 with an Acuson 15L8 transducer.

### Synthesis of PDA NPs

Unfluorinated PDA NPs were synthesized according to a previously reported method.[35] For the synthesis of PDA-174, dopamine hydrochloride (30 mg) was dissolved in a solution of ethanol (20 mL) and water (15 mL) with magnetic stirring. Tris solution (30 mg in 10 mL $H_2O$) was added and the solution was stirred continuously for 24 h at room temperature. The resulting colloidal black suspension was separated by centrifugation and washed with DI water three times. PDA-74 and PDA-350 NPs were prepared similarly with 20 mg and 40 mg of dopamine hydrochloride, respectively.

### Synthesis of PDA-F NPs

For the synthesis of PDA-135-F NPs, dopamine hydrochloride (30 mg) was dissolved in an ethanol (20 mL) and $H_2O$ (15 mL) mixture with magnetic stirring. Tris (30 mg in 10 mL $H_2O$) was added and the system stirred continuously for 9 h. To the resulting black colloidal suspension, 1H,1H,2H,2H-Perfluorodecanethiol (50 μL) was added and stirring was continued for another 15 h. The product was separated by centrifugation and washed with DI water three times. PDA-41-F and PDA-242-F NPs were prepared by identical methods with 20 mg and 40 mg of dopamine hydrochloride, respectively.

### Preparation of PFP loaded PDA and PDA-F NPs

PFP loaded PDA NPs were prepared through a typical immersion method.[33] Particles were freeze dried at −55 °C and 0.04 mbar for 12 h. The subsequent PDA or PDA-F NPs (~1 mg) were dispersed in PFP (200 μL) and sonicated for 30 s. DI water (2 mL) was added to the mixture and another sonication cycle was performed (30 s).

Author Manuscript Author Manuscript Author Manuscript Author Manuscript

### Ultrasound experiments

Aqueous dispersions of PFP-loaded PDA or PDA-F NPs (0.5 mg/mL) were used for all ultrasound experiments. Imaging experiments were performed in both color Doppler and CPS modes. To determine the MI dependence, images were acquired continuously with the increase of MI from 0.06 to 1.9 over the course of 10 s. CPS imaging was performed at 7 MHz and the image brightness was quantified by averaging pixel brightness over the entire sample using Matlab R2016b. Imaging lifetimes were determined by continuous color Doppler imaging at 1.9 MI until the signal fell to the level of the DI water signal intensity.

### Ex vivo porcine liver ultrasound experiments

PFP-loaded PDA-F NPs (4 mg/mL) were injected into fresh pork liver tissue (21 cm×14 cm) with 100 μL volume. Color Doppler images were acquired continuously with the increase of MI from 0.06 to 1.9 immediately after injection. Signal acquisition across MI range allows for the determination of the minimum MI required to generate color Doppler signal in tissue.

### In vitro cytotoxicity assay

In vitro cytotoxicity of PDA-F was performed on HCT116 cell lines using the MTS assay. HCT116 colorectal carcinoma cells were plated at $2.5 \times 10^3$ cells/well in DMEM (Eagle's minimal essential medium) high glucose (Corning) + 10% FBS (fetal bovine serum). Cell were grown for 24 h and then treated with aqueous suspensions of PDA-F ($c$ = 0 to 500 μg/mL). After incubation for 24 h, cells were washed twice with PBS (phosphate-buffered saline) and additional medium (100 μL) was added to each well, followed by CellTiter Aqueous One Solution (Promega, 20 μL). After 3 h at 37 °C, the number of viable cells was determined by comparison of absorbance readings at $\lambda$ = 490 nm (test wavelength) and $\lambda$ = 690 nm (reference wavelength).

## Supplementary Material

Refer to Web version on PubMed Central for supplementary material.

## Acknowledgements

The authors acknowledge generous support from Air Force Office of Scientific Research MURI FA9550–18-1–0142. The authors also acknowledge Dr. Michael D. Burkart at UCSD for assistance with the cell experiments and Dr. Nathan C. Gianneschi at Northwestern University, Dr. Andrew C. Kummel at UCSD for advice and discussions related to the manuscript. The user facilities provided by the National Center for Microscopy and Imaging Research (NCMIR) and Nano3 were utilized for this work.

## References

1. Yildirim A, Chattaraj R, Blum NT, Goldscheitter GM and Goodwin AP, Adv. Healthcare Mater, 2016, 5, 1290–1298.
2. Schutt EG, Klein DH, Mattrey RM and Riess JG, Angew. Chem., Int. Ed, 2003, 42, 3218–3235.
3. Lindner JR, Nat. Rev. Drug Discovery, 2004, 3, 527. [PubMed: 15173842]
4. Szabo TL, Diagnostic ultrasound imaging: inside out, Academic Press, 2nd edn., 2013.
5. Lo AH, Kripfgans OD, Carson PL, Rothman ED and Fowlkes JB, IEEE Transactions on Ultrasonics, Ferroelectrics, and Frequency Control, 2007, 54, 933–946.

Author Manuscript Author Manuscript Author Manuscript Author Manuscript


6. Fabiilli ML, Haworth KJ, Fakhri NH, Kripfgans OD, Carson PL and Fowlkes JB, IEEE Transactions on Ultrasonics, Ferroelectrics, and Frequency Control, 2009, 56, 1006–1017.
7. Wang J, Barback CV, Ta CN, Weeks J, Gude N, Mattrey RF, Blair SL, Trogler WC, Lee H and Kummel AC, IEEE Trans. Med. Imaging, 2017, 37, 222–229. [PubMed: 28829305]
8. Liberman A, Wang J, Lu N, Viveros RD, Allen CA, Mattrey RF, Blair SL, Trogler WC, Kim MJ and Kummel AC, Adv. Funct. Mater, 2015, 25, 4049–4057. [PubMed: 26955300]
9. Wang X, Chen H, Chen Y, Ma M, Zhang K, Li F, Zheng Y, Zeng D, Wang Q and Shi J, Adv. Mater, 2012, 24, 785–791. [PubMed: 22223403]
10. Chen Y, Chen H, Sun Y, Zheng Y, Zeng D, Li F, Zhang S, Wang X, Zhang K, Ma M, He Q, Zhang L and Shi J, Angew. Chem., Int. Ed, 2011, 50, 12505–12509.
11. Ma M, Xu H, Chen H, Jia X, Zhang K, Wang Q, Zheng S, Wu R, Yao M, Cai X, Li F and Shi J, Adv. Mater, 2014, 26, 7378–7385. [PubMed: 25228225]
12. An L, Hu H, Du J, Wei J, Wang L, Yang H, Wu D, Shi H, Li F and Yang S, Biomaterials, 2014, 35, 5381–5392. [PubMed: 24703718]
13. Wang X, Chen H, Zhang K, Ma M, Li F, Zeng D, Zheng S, Chen Y, Jiang L, Xu H and Shi J, Small, 2014, 10, 1403–1411. [PubMed: 24288148]
14. Wang X, Chen H, Zheng Y, Ma M, Chen Y, Zhang K, Zeng D and Shi J, Biomaterials, 2013, 34, 2057–2068. [PubMed: 23246067]
15. Yildirim A, Chattaraj R, Blum NT and Goodwin AP, Chem. Mater, 2016, 28, 5962–5972. [PubMed: 28484307]
16. Wu H, Shi H, Zhang H, Wang X, Yang Y, Yu C, Hao C, Du J, Hu H and Yang S, Biomaterials, 2014, 35, 5369–5380. [PubMed: 24709520]
17. Feng Q, Zhang W, Yang X, Li Y, Hao Y, Zhang H, Hou L and Zhang Z, Adv. Healthcare Mater, 2017, 7, 1700957-n/a.
18. Jia X, Cai X, Chen Y, Wang S, Xu H, Zhang K, Ma M, Wu H, Shi J and Chen H, ACS Appl. Mater. Interfaces, 2015, 7, 4579–4588. [PubMed: 25646576]
19. Min HS, Son S, Lee TW, Koo H, Yoon HY, Na JH, Choi Y, Park JH, Lee J, Han MH, Park R-W, Kim I-S, Jeong SY, Rhee K, Kim SH, Kwon IC and Kim K, Adv. Funct. Mater, 2013, 23, 5518–5529.
20. Liu Y, Ai K and Lu L, Chem. Rev, 2014, 114, 5057–5115. [PubMed: 24517847]
21. Wang Z, Carniato F, Xie Y, Huang Y, Li Y, He S, Zang N, Rinehart JD, Botta M and Gianneschi NC, Small, 2017, 13, 1701830-n/a.
22. Wu Q, Niu M, Chen X, Tan L, Fu C, Ren X, Ren J, Li L, Xu K, Zhong H and Meng X, Biomaterials, 2018, 162, 132–143. [PubMed: 29448141]
23. Ju K-Y, Lee JW, Im GH, Lee S, Pyo J, Park SB, Lee JH and Lee J-K, Biomacromolecules, 2013, 14, 3491–3497. [PubMed: 23987128]
24. Casula MF, Conca E, Bakaimi I, Sathya A, Materia ME, Casu A, Falqui A, Sogne E, Pellegrino T and Kanaras AG, Phys. Chem. Chem. Phys, 2016, 18, 16848–16855. [PubMed: 27282828]
25. Ge R, Lin M, Li X, Liu S, Wang W, Li S, Zhang X, Liu Y, Liu L, Shi F, Sun H, Zhang H and Yang B, ACS Appl. Mater. Interfaces, 2017, 9, 19706–19716. [PubMed: 28553876]
26. Wang Z, Xie Y, Li Y, Huang Y, Parent LR, Ditri T, Zang N, Rinehart JD and Gianneschi NC, Chem. Mater, 2017, 29, 8195–8201.
27. Li Y, Xie Y, Wang Z, Zang N, Carniato F, Huang Y, Andolina CM, Parent LR, Ditri TB, Walter ED, Botta M, Rinehart JD and Gianneschi NC, ACS Nano, 2016, 10, 10186–10194. [PubMed: 27802021]
28. Cui J, Yan Y, Such GK, Liang K, Ochs CJ, Postma A and Caruso F, Biomacromolecules, 2012, 13, 2225–2228. [PubMed: 22792863]
29. Chen X, Yan Y, Müllner M, van Koeverden MP, Noi KF, Zhu W and Caruso F, Langmuir, 2014, 30, 2921–2925. [PubMed: 24597595]
30. Liu Y, Ai K, Liu J, Deng M, He Y and Lu L, Adv. Mater, 2013, 25, 1353–1359. [PubMed: 23280690]
31. Miao Z-H, Wang H, Yang H, Li Z-L, Zhen L and Xu C-Y, ACS Appl. Mater. Interfaces, 2015, 7, 16946–16952. [PubMed: 26196160]

Author Manuscript Author Manuscript Author Manuscript Author Manuscript


32. Huang Y, Vezeridis AM, Wang J, Wang Z, Thompson M, Mattrey RF and Gianneschi NC, J. Am. Chem. Soc, 2017, 139, 15–18. [PubMed: 28032757]
33. Picheth G, Houvenagel S, Dejean C, Couture O, Alves de Freitas R, Moine L and Tsapis N, Acta Biomater, 2017, 64, 313–322. [PubMed: 28986300]
34. Astafyeva K, Somaglino L, Desgranges S, Berti R, Patinote C, Langevin D, Lazeyras F, Salomir R, Polidori A, Contino-Pepin C, Urbach W and Taulier N, J. Mater. Chem. B, 2015, 3, 2892–2907.
35. Yue Q, Wang M, Sun Z, Wang C, Wang C, Deng Y and Zhao D, J. Mater. Chem. B, 2013, 1, 6085–6093.
36. Xu LQ, Yang WJ, Neoh K-G, Kang E-T and Fu GD, Macromolecules, 2010, 43, 8336–8339.
37. Cao Y, Zhang X, Tao L, Li K, Xue Z, Feng L and Wei Y, ACS Appl. Mater. Interfaces, 2013, 5, 4438–4442. [PubMed: 23593981]
38. Zhang L, Wu J, Wang Y, Long Y, Zhao N and Xu J, J. Am. Chem. Soc, 2012, 134, 9879–9881. [PubMed: 22656181]
39. Wang B, Liu Y, Zhang Y, Guo Z, Zhang H, Xin JH and Zhang L, Adv. Mater. Interfaces, 2015, 2, 1500234-n/a.
40. Veith GM and Dudney NJ, J. Electrochem. Soc, 2011, 158, A658–A663.
41. Deshpande N, Needles A and Willmann JK, Clin. Radiol, 2011, 65, 567–581.
42. Garg S, Thomas AA and Borden MA, Biomaterials, 2013, 34, 6862–6870. [PubMed: 23787108]
43. Liberman A, Martinez HP, Ta CN, Barback CV, Mattrey RF, Kono Y, Blair SL, Trogler WC, Kummel AC and Wu Z, Biomaterials, 2012, 33, 5124–5129. [PubMed: 22498299]
44. Longmire M, Choyke PL and Kobayashi H, Nanomed, 2008, 3, 703–717.

Author Manuscript Author Manuscript Author Manuscript Author Manuscript

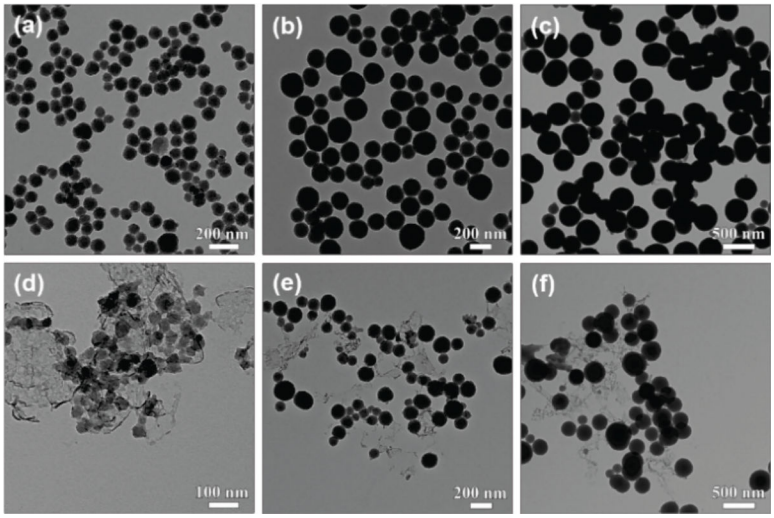


**Fig. 1.**

TEM images of (a) PDA-74, (b) PDA-174, (c) PDA-350, (d) PDA-41-F, (e) PDA-135-F, and (f) PDA-242-F.

Author Manuscript Author Manuscript Author Manuscript Author Manuscript

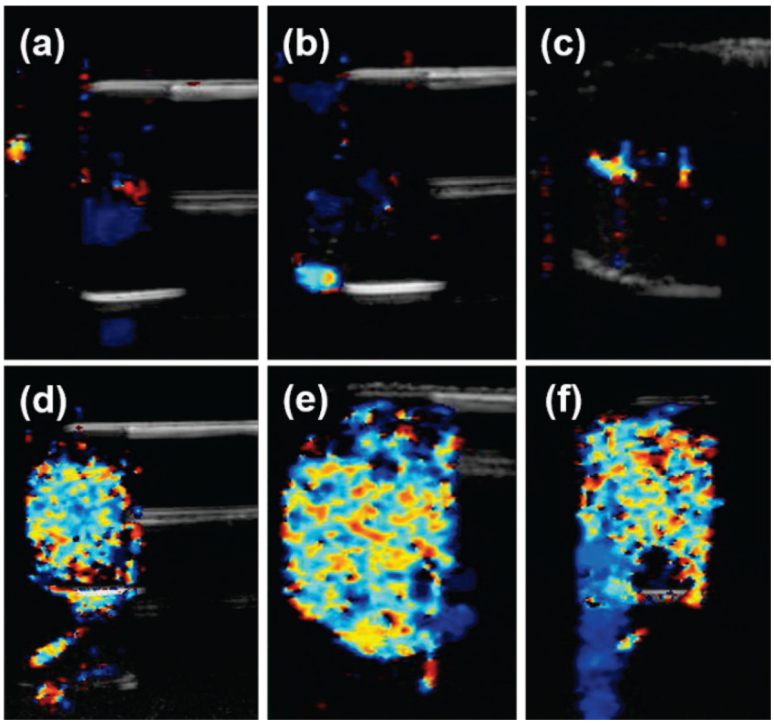


**Fig. 2.**
Color Doppler imaging of (a) PDA-74, (b) PDA-174, (c) PDA-350, (d) PDA-41-F, (e) PDA-135-F, and (f) PDA-242-F at MI=1.9.

Author Manuscript Author Manuscript Author Manuscript Author Manuscript

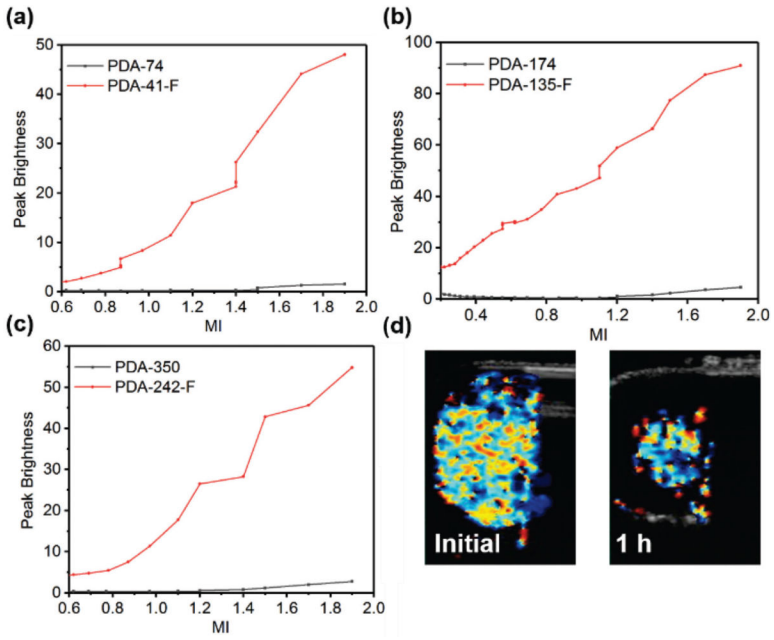


**Fig. 3.**

Quantitative plot of brightness on CPS imaging versus MI for (a) PDA-74 & PDA-41-F, (b) PDA-174 & PDA-135-F, (c) PDA-350 & PDA-242-F, (d) Color Doppler signal detected at (a) beginning and 1 h for PDA-135-F

Author Manuscript Author Manuscript Author Manuscript Author Manuscript

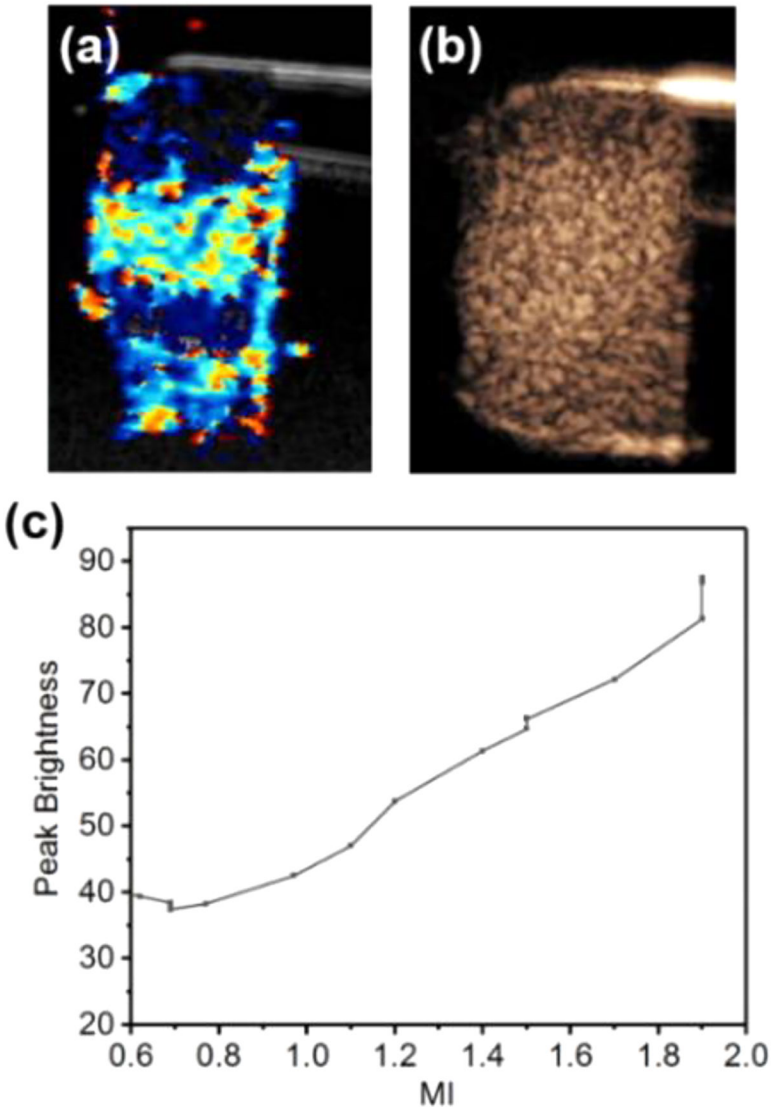


**Fig. 4.**

One-week shelf life test of PDA-135-F for (a) Color Doppler imaging, (b) CPS imaging, and (c) quantitative plot on brightness of CPS imaging versus MI.

Author Manuscript Author Manuscript Author Manuscript Author Manuscript

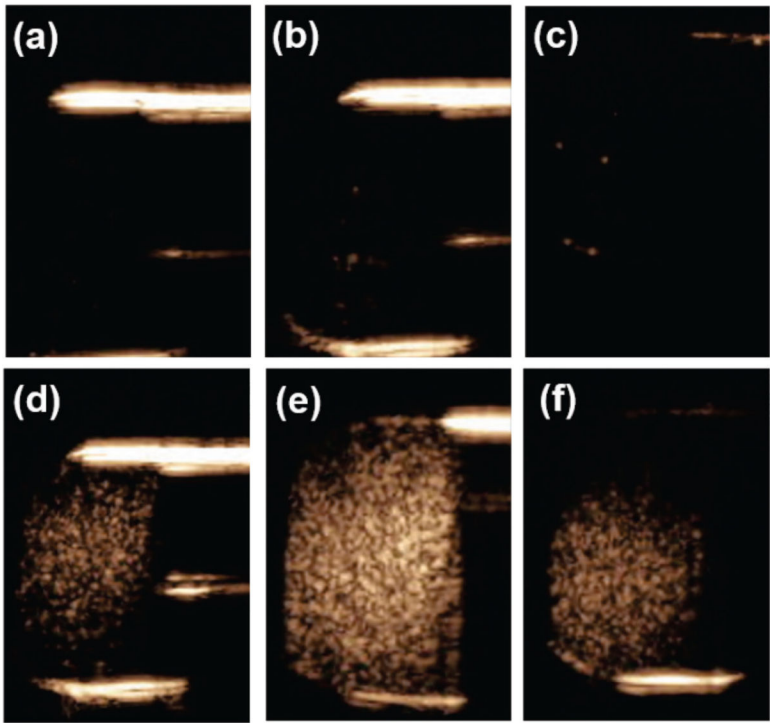


**Fig. 5.**

CPS imaging of (a) PDA-74, (b) PDA-174, (c) PDA-350, (d) PDA-41-F, (e) PDA-135-F, and (f) PDA-242-F at MI=1.9.

Author Manuscript Author Manuscript Author Manuscript Author Manuscript

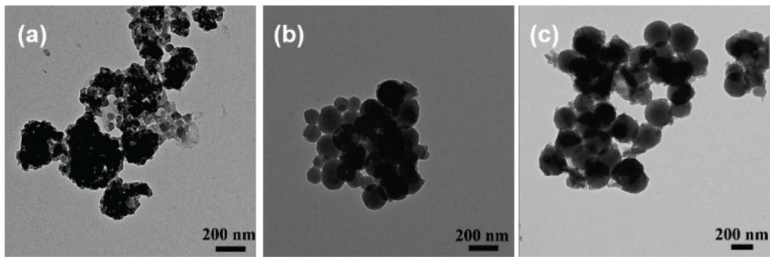


**Fig. 6.**

TEM of PDA-F samples after ultrasound imaging measurement for (a) PDA-41-F, (b) PDA-135-F, and (c) PDA-242-F at MI=1.9

Author Manuscript Author Manuscript Author Manuscript Author Manuscript

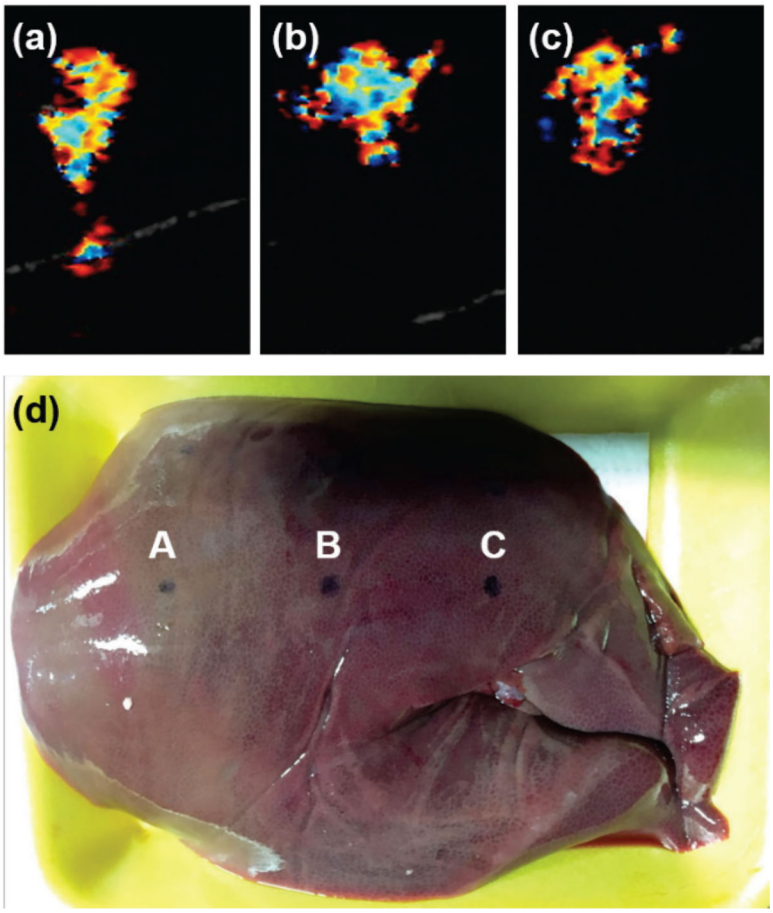


**Fig. 7.**

Color Doppler imaging of (a) PDA-41-F, (b) PDA-135-F, (c) PDA-242-F in fresh porcine liver at MI=1.9. (d) The photograph of the fresh pork liver; PDA-41-F, PDA-135-F, and PDA-242-F was injected into the position of A, B, C, respectively.